Plant Science 266 (2018) 46–54

Contents lists available at ScienceDirect

Plant Science

journal homepage: www.elsevier.com/locate/plantsci

A catechol oxidase AcPPO from cherimoya (*Annona cherimola* Mill.) is localized to the Golgi apparatus

Patricio Olmedo[a], Adrián A. Moreno[a], Dayan Sanhueza[a], Iván Balic[b], Christian Silva-Sanzana[a], Baltasar Zepeda[a], Julian C. Verdonk[c], César Arriagada[d], Claudio Meneses[a], Reinaldo Campos-Vargas[a,*]

[a] Centro de Biotecnología Vegetal, Facultad de Ciencias Biológicas, Universidad Andres Bello, República 217, Santiago, Chile
[b] Departamento de Acuicultura y Recursos Agroalimentarios, Universidad de Los Lagos, Fuchslocher 1305, Osorno, Chile
[c] Horticulture and Product Physiology, Wageningen University, Droevendaalsesteeg 1, 6708 PD Wageningen, The Netherlands
[d] Laboratorio Biorremediación, Departamento de Ciencias Forestales, Facultad de Ciencias Agropecuarias y Forestales, Universidad de La Frontera, Francisco Salazar1145, Temuco, Chile

ARTICLE INFO

Keywords:
Annonaceae
Polyphenol oxidase
Secretory pathway

ABSTRACT

Cherimoya (*Annona cherimola*) is an exotic fruit with attractive organoleptic characteristics. However, it is highly perishable and susceptible to postharvest browning. In fresh fruit, browning is primarily caused by the polyphenol oxidase (PPO) enzyme catalyzing the oxidation of o-diphenols to quinones, which polymerize to form brown melanin pigment. There is no consensus in the literature regarding a specific role of PPO, and its subcellular localization in different plant species is mainly described within plastids. The present work determined the subcellular localization of a PPO protein from cherimoya (AcPPO). The obtained results revealed that the AcPPO- green fluorescent protein co-localized with a Golgi apparatus marker, and AcPPO activity was present in Golgi apparatus-enriched fractions. Likewise, transient expression assays revealed that AcPPO remained active in Golgi apparatus-enriched fractions obtained from tobacco leaves. These results suggest a putative function of AcPPO in the Golgi apparatus of cherimoya, providing new perspectives on PPO functionality in the secretory pathway, its effects on cherimoya physiology, and the evolution of this enzyme.

1. Introduction

The *Annonaceae* family is comprised of more than 100 genera and 2400 species [1]. The cherimoya (*Annona cherimola* Mill.), the most cultivated species of this family [2], is an exotic subtropical fruit native to South America [3]. The organoleptic characteristics of this fruit make it very attractive for use in fresh-cuts, but, like many other fruits, the cherimoya is extremely susceptible to browning caused mainly by polyphenol oxidase (PPO) enzyme activity [4]. This browning reduces the nutritional and sensory properties valued in this fresh fruit [5]. Therefore, study of cherimoya PPO function is of great importance to the fruit industry.

Polyphenol oxidases, classified according to tyrosinase or catecholase activity, are copper-containing enzymes that catalyze the oxidation of different plant metabolites [6–10]. Cherimoya PPO (AcPPO) catalyzes two different reactions, the hydroxylation of monophenols to diphenols and the oxidation of these diphenols to quinones in the presence of oxygen, which spontaneously polymerize to form melanin pigments [11,12]. The role of PPO in plants remains unclear, but PPO has been largely associated with plant defense systems against pathogens and herbivores [13–17]. Polyphenol oxidase has also been related to oxidative stress protection [18], cellular differentiation [19,20], fermentation [21], and protein preservation [22,23].

Protein function is closely related to localization within the cell. Plant PPOs are nuclear-encoded proteins, and most PPOs have an N-terminal chloroplast transit peptide that targets them to the thylakoid lumen [24–26]. However, there are examples of PPO proteins existing in other organelles, such as the vacuole. Specific exceptions include PtrPPO13 from *Populus trichocarpa* and aureusidin synthase 1, a PPO-like protein from *Antirrhinum majus*. These vacuolar PPOs are directed

Abbreviations: AcPPO, *Annona cherimola* polyphenol oxidase; BFA, brefeldin A; BiP, binding immunoglobulin protein; CEF, chloroplast enriched fraction; GEF, Golgi-enriched fraction; GFP, green fluorescent protein; PCC, Pearson's correlation coefficient; PPO, polyphenol oxidase; RGP1, reversibly glycosylated peptide 1; SDS, sodium dodecyl sulfate

* Corresponding author.
E-mail addresses: pa.olmedo@gmail.com (P. Olmedo), amovil@gmail.com (A.A. Moreno), dayansanhueza@gmail.com (D. Sanhueza), ivanbalicnor@gmail.com (I. Balic), c.silva.sanzana@gmail.com (C. Silva-Sanzana), baltasar_zepeda@hotmail.com (B. Zepeda), julian.verdonk@wur.nl (J.C. Verdonk), cesar.arriagada@ufrontera.cl (C. Arriagada), claudio.meneses@unab.cl (C. Meneses), reinaldocampos@unab.cl (R. Campos-Vargas).

http://dx.doi.org/10.1016/j.plantsci.2017.10.012
Received 15 September 2017; Received in revised form 18 October 2017; Accepted 20 October 2017
Available online 05 November 2017
0168-9452/

by an N-terminal signal peptide to the secretory pathway and, ultimately, the vacuole [27,28]. Recently, Tran et al. [29] suggested that several plant PPO genes also possess a signal peptide instead of a chloroplast transit peptide, but the subcellular localization of these genes remains undetermined.

Currently, AcPPO is the only PPO gene cloned from *A. cherimola,* and it is predominantly expressed in the leaves, although it is also present in flowers and fruit tissue [4]. This study characterized a Golgi apparatus-localized PPO from *A. cherimola* using a combined biochemical and confocal microscopy approach.

2. Materials and methods

2.1. Plants

Cherimoya (*A. cherimola* 'Concha Lisa') leaves were collected from adult plants grown in a greenhouse on a 16:8 h light:dark cycle at 21 °C. *Nicotiana benthamiana* plants were grown for 3–4 weeks in a greenhouse on a 16:8 light:dark cycle at 21 °C.

2.2. Cloning of full length AcPPO cDNA

A. cherimola leaves were individually ground to a fine powder in a mortar containing liquid nitrogen. Using the cetrimonium bromide protocol [30,31], total RNA was isolated from 1 g of tissue. RNA integrity was verified on a 1.2% (w/v) agarose gel under denaturing conditions. RNA quality and concentration were measured according to spectrophotometric absorbance at 260 and 280 nm. After treatment with DNase I (Invitrogen™, Carlsbad, CA, USA), cDNA was generated from 1 μg of total RNA by reverse transcription using the Super Script II First-Strand Synthesis System (Invitrogen™, Carlsbad, CA, USA). The polymerase chain reaction was performed using primers for the full-length PPO coding sequence without the stop codon: forward primer 5′-ATGGGACGACCAAGGCTACAG-3′ and reverse primer 5′-CCGCATGTATTCAACGCGTATCC-3′ (GenBank Accession No. DQ990911.1). The polymerase chain reaction product was cloned into the pGEM®-T Easy Vector System (Promega Corp., Madison, WI, USA) and sequenced (Macrogen Inc., Seoul, Korea).

2.3. Plasmid construction and transient expression assay

The AcPPO coding sequence was fused to the green fluorescent protein (GFP) by C-terminal fusion into the pGWB505 binary plant vector under the expression of the 35S promoter [32]. Organelle markers that target the Golgi apparatus (α-1,2 mannosidase 1 [Man1]) and endoplasmic reticulum (wall associated kinase 2 [WAK2]) were used, as described in Nelson et al. [33]. A transient expression assay was carried out as described in Sparkes et al. [34] using *N. benthamiana* leaves 48 h after *Agrobacterium*-mediated infiltration. Brefeldin A treatment was performed as described by Baldwin et al. [35]. Confocal fluorescent images were obtained using an IX 81 inverted microscope (Olympus Corp., Tokyo, Japan) coupled with a FluoView FV 1000 confocal laser scanning microscope with a UPLSAPO 60X NA: 1.35 objective (Olympus Corp., Tokyo, Japan). The colocalization index is represented by Pearson's correlation coefficient calculated as described in [36] using the Jacop plug-in from ImageJ software.

2.4. Computational analysis of AcPPO sequence

Signal peptide prediction was conducted using the bioinformatics tools SignalP 4.1 Server (http://www.cbs.dtu.dk/services/SignalP/) [37] and iPSORT Prediction (http://ipsort.hgc.jp/) [38]. Analysis of subcellular localization was carried out using the TargetP 1.1 Server (http://www.cbs.dtu.dk/services/TargetP/) [39], MultiLoc (https://abi.inf.uni-tuebingen.de/Services/MultiLoc) [40] and ChloroP 1.1 Server (http://www.cbs.dtu.dk/services/ChloroP/) [41]. The transmembrane domain was predicted using the TMHMM 2.0 Server (http://www.cbs.dtu.dk/services/TMHMM-2.0/) [42]. A glycosylation analysis was performed using NetNGlyc 1.0 Server (http://www.cbs.dtu.dk/services/NetNGlyc/) for *N*-glycosylation and using and NetOGlyc 4.0 Server (http://www.cbs.dtu.dk/services/NetOGlyc/) for *O*-glycosylation [43].

2.5. Subcellular fractionation and enrichment for Golgi apparatus vesicles

Fractionation and enrichment of Golgi apparatus vesicles derived from *A. cherimola* and *N. benthamiana* leaves were conducted as described by Muñoz et al. [44] with some modifications. Briefly, fresh leaves were homogenized by a blender and in the presence of 0.5 M sucrose, 100 mM Tris-HCl (pH 7.5), and 5 mM $MgCl_2$, obtaining a crude extract (CE). The suspension was filtered through two layers of gauze and Miracloth (EMB Millipore, Billerica, MA, USA), and chloroplasts and nuclei were sedimented for 20 min at 1000 × *g* by a fixed-angle rotor. The supernatant was loaded onto a 1.3 M sucrose, 100 mM Tris-HCl (pH 7.5), and 5 mM $MgCl_2$ cushion and centrifuged for 100 min at 100,000 × *g* by a swinging bucket rotor. The upper phase was discarded without disturbing the interphase fraction, and sucrose layers of 1.1 M and 0.25 M were overlaid on the membrane pad. The gradient was then centrifuged for 100 min at 100,000 x *g* by a swinging bucket rotor. Fractions of 250 μL were collected from the top of the gradient and used in enzymatic and immunodetection assays.

2.6. PPO activity

Polyphenol oxidase activity was assayed using pyrocatechol as a substrate, following an adapted procedure from Prieto et al. [4]. The reaction mixture contained 50 mM phosphate buffer (pH 6.5) and 20 mM pyrocatechol. Quinone formation was measured in a spectrophotometer at 420 nm for 3 min. Units for PPO activity corresponded to 0.001 absorbance value changes under these conditions.

2.7. PPO activity inhibition and activation assay

The inhibitory dose-response curve was constructed using 1, 5, 10, 25, 50, 100, and 200 μM tropolone (Sigma-Aldrich, St. Louis, MO, USA), and PPO activity was measured as described above. The inhibition assays were performed using Golgi-enriched fractions (GEFs) from *A. cherimola* and *N. benthamiana* expressing AcPPO:GFP leaves. GEFs from control *N. benthamiana* and heat denatured GEFs from *N. benthamiana* expressing AcPPO:GFP were utilized as a negative control. Additionally, PPO activity was measured in absence of pyrocatechol as substrate. PPO activation was carried out using sodium dodecyl sulfate (SDS) [45] and PPO activity was measured as described above plus the addition of 0.1% (w/v) of SDS.

2.8. Measurement of enzyme activity markers

The activity of UDPase, a Golgi apparatus marker, was assayed as described by Nagahashi et al. [46] with modifications. Briefly, a solution containing 6 mM UDP, 6 mM $MgSO_4$, 0.1% (v/v) Triton X-100, and 60 mM Tris-MES (pH 6.5) was mixed with an equal volume of fraction. The released inorganic phosphate was measured at 650 nm according to the method described by Ames [47].

The activity of NADH-cytochrome c oxidoreductase, a mitochondria marker, was measured as described in Wienecke et al. [48] with modifications. For this, the reaction assay mix contained 20 mM phosphate buffer (pH 7.2), 0.02 mM cytochrome c, 0.2 mM NADH, 0.4 mM sodium dithionite, and 0.04% (v/v) Triton X-100. The absorbance decrease at 550 nm was measured by a spectrophotometer for 3 min. In turn, the activity of hydroxypyruvate reductase, a peroxisome marker, was measured as described in Titus et al. [49] with modifications. The assay mixture contained 60 mM phosphate buffer (pH 6.2), 0.2 mM NADH,

0.5 mM lithium-β-hydroxypyruvate, and 0.016% (v/v) Triton X-100. NADH oxidation was measured as the change in absorption at 340 nm for 3 min. The units for cytochrome c oxidoreductase and hydroxypyruvate reductase activities were defined as 0.001 absorbance values changes under the conditions described above.

Chlorophyll *a* and *b* concentrations were determined as detailed in Schaller and DeWitt [50]. Protein quantification was measured as described in Smith et al. [51] using the Pierce™ BCA Protein Assay Kit (Thermo Fischer Scientific Inc., Waltham, MA, USA).

2.9. Immunoblot analysis

This study used an antibody against reversibly glycosylated peptide 1 (RGP1) as a Golgi apparatus marker [52]. An antibody against immunoglobulin binding protein (BiP) was used as an endoplasmic reticulum marker [53] and an antibody against green fluorescent protein (GFP). Immunoblot detection was performed as follows: fractions obtained from the subcellular fractionation using *A. cherimola* or *N. benthamiana* expressing AcPPO:GFP or non-transformed *N. benthamiana* leaves were homogenized in SDS loading buffer (125 mM Tris-HCl [pH 6.8], 4% (w/v) SDS, 20% (v/v) glycerol, 0.02% (w/v) bromophenol blue, and 10% β-mercaptoethanol) and heated at 100 °C for 10 min. Then, 20 µL aliquots were loaded on gel for immunoblotting [54]. Immunoblots were probed with a 1:5000 dilution of the anti-RGP1 antibody [55], anti-BiP antibody (ADI-SPA-818-F; Enzo Life Sciences, Inc.) and anti-GFP antibody (AbID ab6556, Abcam) followed by incubation in a 1:5000 dilution of a horseradish peroxidase-conjugated goat anti-rabbit or −mouse antibody (KPL 074-1506; KPL 074-1806). The secondary antibody was visualized by a SuperSignal™ West Pico Chemiluminescent Substrate Kit (Pierce Biotechnology Inc., Rockford, IL, USA).

2.10. PPO topology analysis

Topological analysis of AcPPO was performed as outlined by Connolly et al. [56] with modifications. Intact Golgi apparatus vesicles from *A. cherimola* and the *Agrobacterium*-mediated transient expression of AcPPO:GFP in *N. benthamiana* leaves were incubated for 30 min at room temperature in the presence or absence of 1% Triton X-100. For proteinase K treatment, the Golgi vesicles were incubated for 60 min at 37 °C in the presence or absence of 4 µg of proteinase K. Polyphenol oxidase activity was measured as described above.

2.11. Subcellular fractionation and enrichment for chloroplasts

Fractionation and enrichment of chloroplasts derived from *A. cherimola* leaves were conducted as described by Nishimura et al. [57] and Takabe et al. [58] with modifications. Briefly, fresh leaves were homogenized by a blender and in the presence of 0.5 M sucrose, 100 mM Tris-HCl (pH 7.5), and 5 mM $MgCl_2$. The suspension was filtered through two layers of gauze and Miracloth (EMB Millipore, Billerica, MA, USA), 1 mL of the filtered solution was loaded onto 3 mL of a linear sucrose gradient (11%–90% w/v) dissolved in 0.02 M Tricine-KOH (pH = 7.5) and centrifuged for 120 min at 6650 × *g* by a swinging bucket rotor at 4 °C. Fractions of 250 µL were collected from the top of the gradient, obtaining a chloroplast-enriched fractions (CEF) that were used in enzymatic assays.

2.12. Statistical analysis

Statistical analysis was performed using analysis of variance, and mean comparisons between treatments were determined using Tukey's test at $p < 0.05$. These analyses were carried out using the R statistical analysis package v.3.0.1. (http://www.R-project.org, R Foundation for Statistical Computing, Vienna, Austria). Experiments were carried out using three biological replicates with three technical replicates.

Table 1
Computational analysis of AcPPO sequence. SignalP 4.1 Server[a], iPSORT Server[b], ChloroP 1.1 Server[c], TargetP 1.1 Server[d], MultiLoc Server[e] and TMHMM 2.0 Server[f].

	GenBank	*Signal Peptide*	*Chloroplast Signal*	*Predicted Location*	*Transmembrane Domain*
AcPPO	DQ990911.1	Yes[a] [37] – Yes[b] [38]	No[c] [41]	Secretory Pathway[d] [39] – Golgi Apparatus[e] [40]	No[f] [42]

3. Results

3.1. Subcellular localization of AcPPO in N. benthamiana leaves

To gain a better understanding of *A. cherimola* PPO, the amino acid sequence previously described by Prieto et al. [4] was used to perform an *in silico* analysis using web-based tools as showed in Table 1. The bioinformatics ChloroP Server suggested no direction of AcPPO to chloroplasts, and the SignalP and iPSORT tools indicated the presence of an N-terminal signal peptide in AcPPO. Additionally, the TargetP Server suggested secretory pathway localization based on the N-terminal sequence of AcPPO and a Golgi apparatus localization suggested by the MultiLoc tool. The TMHMM Server indicated no transmembrane domain in the sequence. To obtain additional information about AcPPO, the prediction of glycosylation sites indicated the presence of at least four sites for *N*-glycosylation and twelve sites for *O*-glycosylation in the AcPPO sequence.

To determine AcPPO localization *in vivo*, the coding sequence was cloned and translationally fused to GFP. Transient expression of AcPPO:GFP using *Agrobacterium* infiltration resulted in a punctate fluorescence pattern (Fig. 1A). When this construct was co-infiltrated with a Golgi apparatus marker, a co-localization pattern was observed with a Pearson's correlation coefficient (PCC) equal to 0.67 (Fig. 1B and C). To confirm possible localization of AcPPO:GFP in the Golgi apparatus, *N. benthamiana* leaves expressing this construct were treated with brefeldin A, a drug that inhibits protein transport from the endoplasmic reticulum to the Golgi apparatus [59]. After 60 min of brefeldin A exposure, the punctate pattern that represented Golgi stacks was redistributed into a mesh-like fluorescence pattern that co-localized with an endoplasmic reticulum marker with a PCC equal to 0.85 (Fig. 1D–F). No co-localization of AcPPO:GFP with an endoplasmic reticulum marker was observed in absence of BFA with a PCC equal to 0.15 (Fig. 1G–I). Additionally, transient expression of the AcPPO:GFP in *N. benthamiana* leaves showed no co-localization with the chloroplast marker (chlorophyll autofluorescence) with a PCC equal to 0.06 (Supplementary Figs. S1A-C), suggesting that AcPPO differ from classical plant plastid PPOs.

3.2. Detection of PPO activity in GEFs of A. cherimola leaves

Since AcPPO:GFP was localized in the Golgi apparatus of *N. benthamiana* leaves, the subcellular localization of AcPPO in *A. cherimola* leaves was investigated by sucrose density gradient centrifugation. This technique allows for the separation of the endoplasmic reticulum from Golgi apparatus- and vacuole-enriched fractions [60]. A major peak of AcPPO activity was detected in fraction 3 (Fig. 2A). Moreover, this peak correlated with a peak of UDPase activity (Fig. 2B), a known biomarker for Golgi apparatus as described by Nagahashi et al. [46]. Immunoblot analysis of fractions collected using an anti-RGP1 antibody [52] showed a correlation between AcPPO activity, UDPase activity, and RGP1 detection (Fig. 2C). Immunodetection using an anti-BiP antibody [53] indicated that GEFs still contained endoplasmic reticulum contamination, but no AcPPO activity was detected in endoplasmic reticulum enriched fractions (Fig. 2D). No activity associated with mitochondria and peroxisomes was found, and chlorophyll concentration analysis

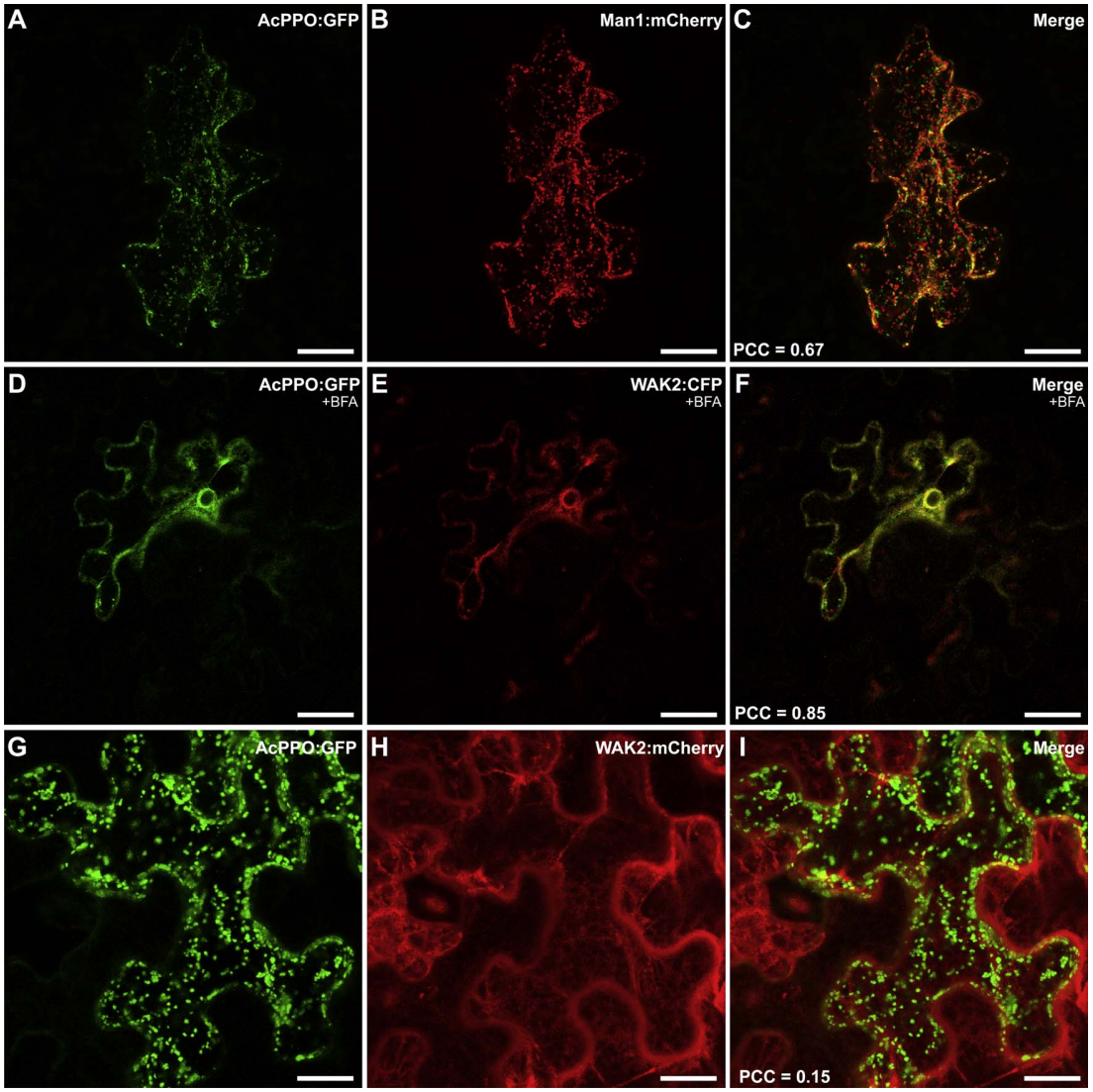

Fig. 1. AcPPO localizes in the Golgi apparatus of *N. benthamiana* leaves. Transient expression of AcPPO:GFP (A) and Golgi apparatus marker, α-1,2-mannosidase-1 (Man1:mCherry) (B) in *N. benthamiana* leaves. Co-localization of AcPPO:GFP and the Golgi apparatus marker (C) was detected. BFA assay using AcPPO:GFP (D) and the endoplasmic reticulum marker, wall associated kinase-2 (WAK2:CFP showed in red) (E). Redistribution of AcPPO:GFP into the endoplasmic reticulum is observed (F). No co-localization was observed of AcPPO:GFP (G) and the ER marker (WAK2:mCherry) (H) in absence of BFA (I). Cells were observed 48 h after infiltration using a confocal laser scanning microscope. Scale bars indicate 20 μm. (For interpretation of the references to colour in this figure legend, the reader is referred to the web version of this article.)

suggested the absence of chloroplasts (Supplementary Figs. S2A and B). Because plant PPOs are mainly localized within the chloroplasts, we determine if the cherimoya leaves contain another chloroplast-located PPOs. A linear sucrose density gradient centrifugation was carried out to obtain chloroplast-enriched fractions (CEFs) using cherimoya leaves. A peak of PPO activity using pyrocatechol as substrate was detected in fraction 7 (Supplementary Fig. S3A). This peak of PPO activity correlates with a mayor peak of chloroplast presence as measured by the chlorophyll a + b content (Supplementary Fig. S3B). Moreover, the PPO activity, measured as latent PPO activity, was activated using 0.1% (w/v) of SDS, showing a significantly increased activity of the cherimoya chloroplast PPO (Supplementary Fig. S3C). As a control, PPO activity was measured in absence of pyrocatechol, showing no activity (Supplementary Fig. S3C). PPO activity and protein content from CEF and GEF was compared, showing that PPOs were present in both organelles, chloroplast and Golgi apparatus (Supplementary Fig. S3D).

3.3. AcPPO activity is conserved in Golgi apparatus fractions of N. benthamiana leaves agroinfiltrated with AcPPO:GFP

To confirm that the protein encoded by the AcPPO gene was responsible for the PPO activity in *A. cherimola* leaves, GEFs were isolated by sucrose density gradient centrifugations of *Agrobacterium*-mediated transient expression of AcPPO:GFP in *N. benthamiana* leaves. As observed in Fig. 2F, the major peak of AcPPO activity was observed in fraction 3. This peak of PPO activity correlated with the maximal UDPase activity detected (Fig. 2G). Moreover, immunodetection of RGP1 showed a similar pattern across the sucrose gradient, supporting the Golgi apparatus localization of AcPPO (Fig. 2H) inferred from the results obtained using *A. cherimola* leaves. Additionally, no AcPPO activity was found in endoplasmic reticulum-enriched fractions assessed by BiP immunodetection assays (Fig. 2I) and immunodetection of GFP showed a correlation with the Golgi markers, suggesting that PPO activity detected is catalyzed by AcPPO:GFP present in these fractions (Fig. 2J). As a control, *A. cherimola* fractions were assessed by GFP immunodetection showing an absence of GFP signal (Fig. 2E). No

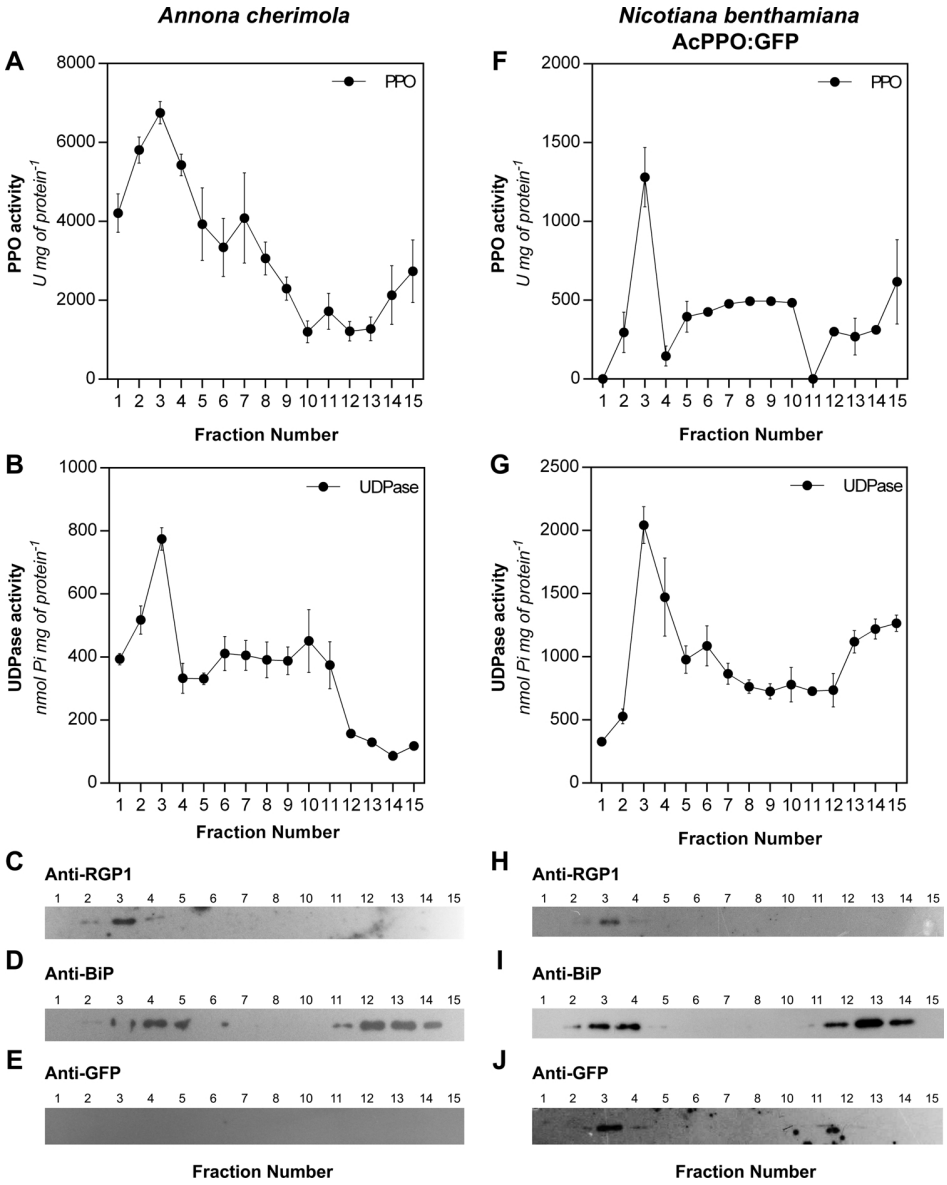

Fig. 2. AcPPO activity is detected in Golgi apparatus fractions of *A. cherimola* and *N. benthamiana* expressing AcPPO:GFP leaves. Leaves were homogenized and organelles were separated in a discontinuous sucrose density gradient, and the aliquots were utilized for different organelle marker activities. *A. cherimola* fractions (A–E) and *N. benthamiana* expressing AcPPO:GFP (F–J). AcPPO activity (PPO) (A and F). UDPase activity (Golgi apparatus marker; UDPase) (B and G). Immunodetection of a Golgi apparatus marker RGP1 (C and H), an endoplasmic reticulum marker BiP (D and I) and GFP (E and J).

mitochondria or peroxisomes marker activities were observed and chlorophyll determination suggested no presence of chloroplasts (Supplementary Figs. S2D and E). Subcellular fractionation of non-transformed *N. benthamiana* leaves showed minimal PPO activity across the gradient and immunodetection of GFP showed an absence of GFP signal (Supplementary Fig. S4).

3.4. AcPPO activity is inhibited by tropolone and activated by SDS

To confirm if the pyrocatechol oxidation observed in the fractionation analysis depended on AcPPO activity, a new PPO activity assay was performed using GEFs in the presence of tropolone, a known inhibitor of PPO activity [61]. A tropolone dose-response curve using GEFs from *A. cherimola* indicated that PPO activity was almost completely inhibited by 200 μM of tropolone (Fig. 3A). Based on this result, the same concentration of tropolone was used in the subsequent reactions. To determine if the observed activity was attributable to enzymatic activity of PPO, AcPPO activity was analyzed using GEFs from *N. benthamiana* leaves agroinfiltrated with AcPPO:GFP in the presence or absence of tropolone or after boiling the extract for 10 min. In the presence of tropolone, PPO activity was observed to decrease to a basal level (Fig. 3B), as occurred in GEFs obtained from *A. cherimola*. Additionally, PPO activity ceased when the GEF extract was boiled. These results suggest that the PPO activity detected in *N. benthamiana* leaves agroinfiltrated with AcPPO:GFP is a product of enzymatic activity and not only a redox reaction.

Following the characterization of this AcPPO enzyme, an activation assay was performed using SDS. PPO activity was measured as latent PPO activity (in absence of SDS) and a significant increase was detected in the presence of 0.1% (w/v) SDS (Fig. 3C). As a control, PPO activity was measured in absence of pyrocatechol, showing no activity (Fig. 3C).

3.5. AcPPO resides in the lumen of the Golgi apparatus

Since bioinformatic analysis of the AcPPO amino acid sequence suggested a lack of transmembrane domains, it was possible that AcPPO could be a soluble protein within the Golgi apparatus. To test this hypothesis, Golgi vesicles were treated with proteinase K, a protease unable to penetrate intact membranes [62], in the presence or absence of 1% (v/v) Triton X-100. Unexpectedly, significantly increased AcPPO activity was observed in *A. cherimola* GEFs and in *Agrobacterium*-mediated transient expression of AcPPO:GFP in *N. benthamiana* leaves

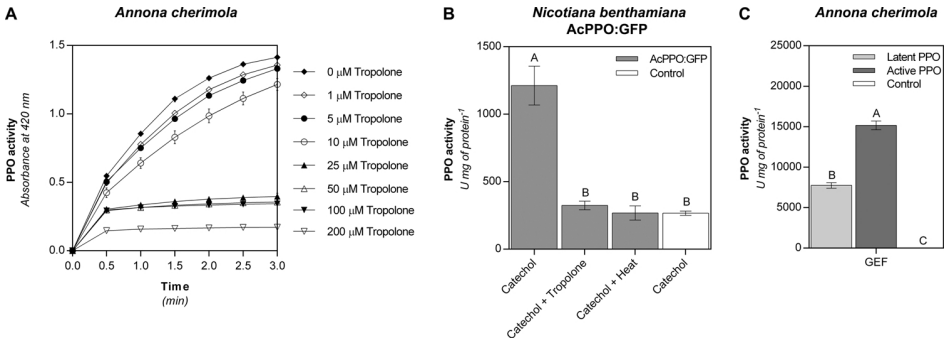

Fig. 3. Tropolone inhibits Golgi apparatus AcPPO activity in a dose-dependent manner. AcPPO activity from *A. cherimola* GEFs measured in a dose-response curve using tropolone as competitor inhibitor (A). Inhibition assay in GEFs from *N. benthamiana* leaves expressing AcPPO:GFP and GEF that were exposed to heat denaturation (B). Non-transformed N. benthamiana leaves are represented as control (B). AcPPO is activated by SDS. GEFs from *A. cherimola* leaves were exposed to 0.1% (w/v) of SDS (Active PPO) (C). AcPPO activity measured in absence of pyrocatechol as substrate is showed as control (C).

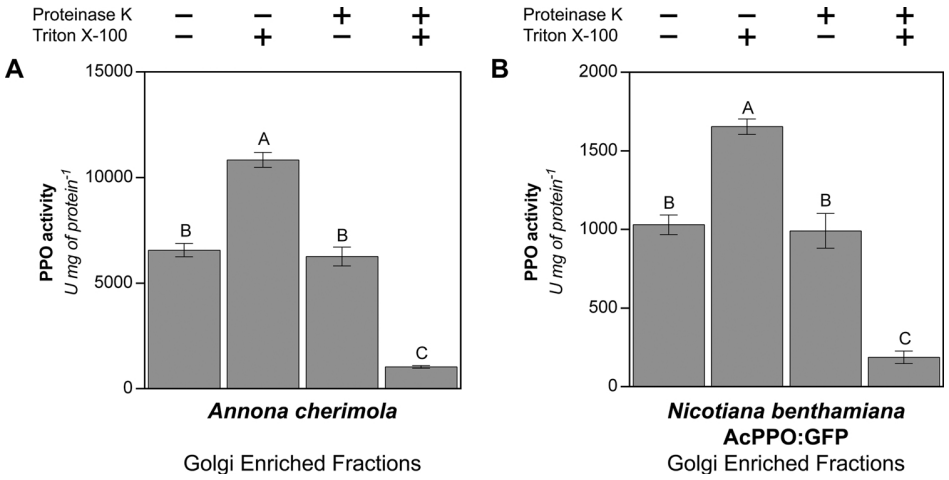

Fig. 4. Topological analysis of AcPPO in GEFs of *A. cherimola* and *N. benthamiana* leaves expressing AcPPO:GFP. AcPPO activity measured in treatments with proteinase K in presence and absence of 1% (v/v) Triton X-100 in *A. cherimola* leaves (A) and *Agrobacterium*-mediated transient expression of AcPPO:GFP in *N. benthamiana* leaves (B).

exposed only to 1% (v/v) Triton X-100 (Fig. 4A and B). This suggests that pyrocatechol entry into the Triton-permeabilized vesicles is a rate limiting factor for the PPO activity in the assessed conditions. However, no alterations of AcPPO activity were observed in GEFs treated with proteinase K in the absence of 1% (v/v) Triton X-100. Nevertheless, and in line with the proposed hypothesis, proteinase K treatment of GEFs exposed to 1% (v/v) Triton X-100 resulted in a significant decrease in AcPPO activity (Figs. 4A and B), suggesting that AcPPO resides in the lumen of the Golgi apparatus.

4. Discussion

Our subcellular localization analyses using confocal microscopy strongly supported that AcPPO is located within the Golgi apparatus. The AcPPO protein tagged with GFP displayed a fluorescence distribution typical of Golgi apparatus-localized proteins [35,63–66], as well as redistribution into aggregated structures in the presence of brefeldin A [67]. However, co-localization of AcPPO:GFP with the Golgi marker α-1,2 mannosidase I (Man1-mCherry) was partially observed. A similar co-localization pattern has been described between a *trans*-Golgi marker and the α-1,2 mannosidase I marker used in this work [68], given the fact that this marker has a *cis*-Golgi localization. These results suggest that the AcPPO:GFP fusion possibly has both, *cis*- and *trans*-Golgi localization, explaining the Pearson's correlation coefficient of 0.67. Additionally, subcellular fractionation showed an overlap between AcPPO activity and Golgi apparatus markers (UDPase activity and RGP1 immunodetection). The AcPPO activity was not caused by endoplasmic reticulum contamination of the Golgi fractions, as endoplasmic reticulum-enriched fractions showed no AcPPO activity. Furthermore, *N. benthamiana* leaves transiently expressing AcPPO:GFP demonstrated the same correlation between AcPPO activity and Golgi apparatus markers in sucrose fractions. This measurement also suggest that AcPPO was correctly processed by the *N. benthamiana* secretory pathway machinery and that GFP fusion did not interfere with protein conformation and AcPPO activity. Moreover, the immunodetection of GFP using sucrose fractions from *N. benthamiana* leaves expressing the AcPPO:GFP fusion strongly support the correlation between the Golgi markers and the AcPPO activity detected, compared with the non-transformed *N. benthamiana* leaves, where minimal PPO activity was observed and no GFP was immunodetected (Supplementary Fig. S3). Thus, the peak of PPO activity measured in *N. benthamiana* leaves expressing the AcPPO:GFP is due to the presence of the AcPPO within the Golgi apparatus.

Cherimoya PPO activity in GEFs and AcPPO:GFP expression in *N. benthamiana* leaves were almost completely inhibited by tropolone, a potent competitive inhibitor of PPOs, tyrosinases and laccases [61,69–71]. Tropolone facilitates the differentiation of PPO from other oxidases, such as peroxidases, indicating that the AcPPO activity reported in this work must be a PPO-derived activity [61]. Furthermore, topological studies of AcPPO using proteinase K and Triton X-100 determined that the AcPPO catalytic domain faces the lumen of the Golgi apparatus. The absence of putative transmembrane domains predicted computationally suggest that AcPPO is a soluble protein within the Golgi apparatus.

Since PPO activity is commonly associated to the chloroplast [29], a sucrose density gradient was carried out to obtain a chloroplast-enriched fraction. In this CEF, a major peak of PPO activity was detected and correlated with the peak of chlorophyll content. Additionally, the AcPPO:GFP was not co-localized with the chloroplast marker (chlorophyll autofluorescence), suggesting that the PPO characterized in this work probably belongs to a PPO family with members localized within the chloroplast in the *A. cherimola* leaves. This observation is in agreement with the PPO gene family in poplar (*P. trichocarpa*), containing fifteen PPO genes, fourteen localized within the chloroplast and one localized within the vacuole [28]. Therefore, *A. cherimola* possess chloroplast- and secretory route localized PPO enzymes.

To our knowledge, this work describes for first time a PPO localized in the Golgi apparatus. Recent reports associated two PPOs with the secretory pathway, specifically with the vacuole. One PPO was *A. majus* aureusidin synthase 1, a flavonoid biosynthetic PPO involved in flower pigmentation that shares 44% of identity with AcPPO [8,27,72]. The other PPO was PtrPPO13, the vacuole-localized PPO from *P. trichocarpa* [28] that has 57% identity with AcPPO, although no function has been associated to this PPO. Similarly, AcPPO also contained a predicted signal peptide in its coding sequence that could drive this PPO to the secretory pathway. Despite these resemblances, the specific function of this PPO is unknown. Tran et al. [29] identified several plant PPO genes encoding for a signal peptide, but only aureusidin synthase 1 (AmAS1) and PtrPPO13 were well described. Curiously, a BLAST search performed using the AcPPO amino acid sequence first received hits for some members of the Eudicot I clade [29] (Supplementary Table S1), suggesting that AcPPO could share a similar origin with non-plastid PPOs and a location divergence during plant evolution. The collected data also suggest that not all the non-plastid PPOs are localized in plant vacuoles and that protein sequences must contain particular signatures to target specific cell compartments. Supplementary Table S1 shows the first ten hits from the BLAST mentioned above, indicating a prediction of the subcellular localization of these PPO proteins using TargetP [39] and MultiLoc [40]. Surprisingly, most of these predictions pointed these PPOs to the secretory pathway within different subcellular localizations, indicating that plant PPO gene families could evolved and change the chloroplast location to obtain specialized metabolic processes.

Several plant PPOs have been characterized and most of them remain with no specific function. However, some PPOs do have a determined role and are related to the oxidation of phenolic compounds in secondary metabolism [73]. Betalain biosynthesis by the oxidation of DOPA to *cyclo*-DOPA are associated to PPO activity in transgenic tobacco cells [74]. Aurone biosynthesis is also mediated by a PPO-like protein in snapdragron [27]. Moreover, tyrosine metabolism has been related to PPO activity by the conversion of tyrosine to L-DOPA in walnut leaves [20]. Additionally, the biosynthesis of 8-8′ linked lignans in creosote bush are mediated by the tyrosinase activity of a PPO [7]. Finally, has been described a laticifer-PPO involved in latex coagulation and wound sealing in dandelion [75]. According to these functions described, we do not discard a putative role of AcPPO in the modification of Golgi-located phenolics and flavonoids. The phenolic compounds are mobilized through vesicle transfer system and membrane-mediated transport, involving the organelles from the plant secretory pathway in a Golgi-independent and Golgi-dependent manner [76–80]. Additionally, hydroxycinnamic acids are located in the Golgi apparatus during monolignol biosynthesis [81] and *p*-coumaric acid, a hydroxycinnamic acid, is hydroxylated to caffeic acid by PPO activity [13]. Moreover, vacuole accumulation of flavonoids requires a Golgi-localized protein [79] and has been described the PPO activity on flavonoids, such chalcones [27]. Furthermore, a proteomic analysis of Arabidopsis Golgi apparatus indicates that 1% of these proteins corresponds to redox enzymes, including oxidoreductases, peroxidases and miscellaneous proteins [82], supporting the hypothesis that AcPPO could have an oxidative role within the *A. cherimoya* Golgi vesicles. However, future studies are needed to continue elucidating possible functions and bioinformatics approaches will support the identification of these specialized PPOs.

Acknowledgment

Fondecyt 1040011, 1150492, 3150538

Appendix A. Supplementary data

Supplementary data associated with this article can be found, in the online version, at http://dx.doi.org/10.1016/j.plantsci.2017.10.012.

References

[1] L.W. Chatrou, M.D. Pirie, R.H.J. Erkens, T.L.P. Couvreur, K.M. Neubig, J.R. Abbott, J.B. Mols, J.W. Maas, R.M.K. Saunders, M.W. Chase, A new subfamilial and tribal classification of the pantropical flowering plant family Annonaceae informed by molecular phylogenetics, Bot. J. Linn. Soc. 169 (2012) 5–40, http://dx.doi.org/10.1111/j.1095-8339.2012.01235.x.

[2] R. Alique, Residual effects of short-term treatments with high CO2 on the ripening of cherimoya (Annona cherimola Mill.) fruit, J. Hortic. Sci. 70 (1995) 609–615 http://search.ebscohost.com/login.aspx?direct=true&db=lah&AN=19950312498&site=ehost-live.

[3] M. van Zonneveld, X. Scheldeman, P. Escribano, M.A. Viruel, P. van Damme, W. Garcia, C. Tapia, J. Romero, M. Sigueñas, J.I. Hormaza, Mapping genetic diversity of cherimoya (Annona cherimola mill.): application of spatial analysis for conservation and use of plant genetic resources, PLoS One 7 (2012), http://dx.doi.org/10.1371/journal.pone.0029845.

[4] H. Prieto, D. Utz, Castro Á, C. Aguirre, M. González-Agüero, H. Valdés, N. Cifuentes, B.G. Defilippi, P. Zamora, G. Zúñiga, R. Campos-Vargas, Browning in Annona cherimola fruit: role of polyphenol oxidase and characterization of a coding sequence of the enzyme, J. Agric. Food Chem. 55 (2007) 9208–9218, http://dx.doi.org/10.1021/jf070586+.

[5] S. Lima De Oliviera, N.B. Guerra, M.I. Sucupira Maciel, A.V. Souza Livera, Polyphenoloxidase activity, polyphenols concentration and browning intensity during soursop (Annona muricata, L.) maturation, J. Food Sci. (1994) 1050–1052, http://dx.doi.org/10.1111/j.1365-2621.1994. tb08187.x.

[6] U. Steiner, W. Schliemann, H. Böhm, D. Strack, Tyrosinase involved in betalain biosynthesis of higher plants, Planta 208 (1999) 114–124, http://dx.doi.org/10.1007/s004250050541.

[7] M.-H. Cho, S.G.A. Moinuddin, G.L. Helms, S. Hishiyama, D. Eichinger, L.B. Davin, N.G. Lewis, (+)-Larreatricin hydroxylase, an enantio-specific polyphenol oxidase from the creosote bush (Larrea tridentata), Proc. Natl. Acad. Sci. U. S. A. 100 (2003) 10641–10646, http://dx.doi.org/10.1073/pnas.1934562100.

[8] E. Ono, M. Fukuchi-Mizutani, N. Nakamura, Y. Fukui, K. Yonekura-sakakibara, M. Yamaguchi, T. Nakayama, T. Tanaka, T. Kusumi, Y. Tanaka, Yellow flowers generated by expression of the aurone biosynthetic pathway, Proc. Natl. Acad. Sci. U. S. A. 103 (2006) 11075–11080, http://dx.doi.org/10.1073/pnas.0604246103.

[9] V.M. Virador, J.P. Reyes Grajeda, A. Blanco-Labra, E. Mendiola-Olaya, G.M. Smith, A. Moreno, J.R. Whitaker, Cloning, sequencing, purification, and crystal structure of grenache (VITIS vinifera) polyphenol oxidase, J. Agric. Food Chem. 58 (2010) 1189–1201, http://dx.doi.org/10.1021/jf902939q.

[10] T. Boeckx, A.L. Winters, K.J. Webb, A.H. Kingston-Smith, Polyphenol oxidase in leaves: is there any significance to the chloroplastic localization? J. Exp. Bot. 66 (2015) 3571–3579, http://dx.doi.org/10.1093/jxb/erv141.

[11] A. Mathew, H. Parpia, Food browing as a polyphenol reaction, Adv. Food Res. 19 (1971) 75–145.

[12] M. Martinez-Cayuela, L. Sanchez de Medina, M.J. Faus, A. Gil, Cherimoya (Annona cherimola Mill,) polyphenoloxidase: monophenolase and dihydroxyphenolase activities, J. Food Sci. 53 (1988) 53–56.

[13] P. Thipyapong, M.D. Hunt, J.C. Steffens, Antisense downregulation of polyphenol oxidase results in enhanced disease susceptibility, Planta 220 (2004) 105–117, http://dx.doi.org/10.1007/s00425-004-1330-6.

[14] L. Li, J.C. Steffens, Overexpression of polyphenol oxidase in transgenic tomato plants results in enhanced bacterial disease resistance, Planta 215 (2002) 239–247, http://dx.doi.org/10.1007/s00425-002-0750-4.

[15] C.P. Constabel, L. Yip, J.J. Patton, M.E. Christopher, Polyphenol oxidase from hybrid poplar. Cloning and expression in response to wounding and herbivory, Plant Physiol. 124 (2000) 285–295, http://dx.doi.org/10.1104/pp.124.1.285.

[16] C.P. Constabel, D.R. Bergey, C.A. Ryan, Systemin activates synthesis of wound-inducible tomato leaf polyphenol oxidase via the octadecanoid defense signaling pathway, Plant Biol. 92 (1995) 407–411, http://dx.doi.org/10.1073/pnas.92.2.407.

[17] P. Thipyapong, J.C. Steffens, Tomato polyphenol oxidase (differential response of the polyphenol oxidase F promoter to injuries and wound signals), Plant Physiol. 115 (1997) 409–418, http://dx.doi.org/10.1104/pp.115.2.409.

[18] T. Boeckx, R. Webster, A.L. Winters, K.J. Webb, A. Gay, A.H. Kingston-Smith, Polyphenol oxidase-mediated protection against oxidative stress is not associated with enhanced photosynthetic efficiency, Ann. Bot. 116 (2015) 529–540, http://dx.doi.org/10.1093/aob/mcv081.

[19] K.J. Webb, A. Cookson, G. Allison, M.L. Sullivan, A.L. Winters, Polyphenol oxidase affects normal nodule development in red clover (Trifolium pratense L.), Front. Plant Sci. 5 (2014) 700, http://dx.doi.org/10.3389/fpls.2014.00700.

[20] S. Araji, T.A. Grammer, R. Gertzen, S.D. Anderson, M. Mikulic-Petkovsek, R. Veberic, M.L. Phu, A. Solar, C.A. Leslie, A.M. Dandekar, M.A. Escobar, Novel roles for the polyphenol oxidase enzyme in secondary metabolism and the regulation of cell death in walnut, Plant Physiol. 164 (2014) 1191–1203, http://dx.doi.org/10.1104/pp.113.228593.

[21] N. Subramanian, P. Venkatesh, S. Ganguli, V.P. Sinkar, Role of polyphenol oxidase and peroxidase in the generation of black tea theaflavins, J. Agric. Food Chem. 47 (1999) 2571–2578, http://dx.doi.org/10.1021/jf981042y.

[22] M.R.F. Lee, A.L. Winters, N.D. Scollan, R.J. Dewhurst, M.K. Theodorou, F.R. Minchin, Plant-mediated lipolysis and proteolysis in red clover with different polyphenol oxidase activities, J. Sci. Food Agric. 84 (2004) 1639–1645, http://dx.doi.org/10.1002/jsfa.1854.

[23] M.L. Sullivan, R.D. Hatfield, Polyphenol oxidase and *o*-diphenols inhibit postharvest proteolysis in red clover and alfalfa, Crop Sci. 46 (2006) 662–670.

[24] A.M. Mayer, Polyphenol oxidases in plants and fungi: going places? A review, Phytochemistry 67 (2006) 2318–2331, http://dx.doi.org/10.1016/j.phytochem.2006.08.006.
[25] P. Thipyapong, M.J. Stout, J. Attajarusit, Functional analysis of polyphenol oxidases by antisense/sense technology, Molecules 12 (2007) 1569–1595, http://dx.doi.org/10.3390/12081569.
[26] S. Koussevitzky, E. Ne'eman, S. Peleg, E. Harel, Polyphenol oxidase can cross thylakoids by both the Tat and the Sec-dependent pathways: a putative role for two stromal processing sites, Physiol. Plant. 133 (2008) 266–277, http://dx.doi.org/10.1111/j.1399-3054.2008.01074.x.
[27] E. Ono, M. Hatayama, Y. Isono, T. Sato, R. Watanabe, K. Yonekura-Sakakibara, M. Fukuchi-Mizutani, Y. Tanaka, T. Kusumi, T. Nishino, T. Nakayama, Localization of a flavonoid biosynthetic polyphenol oxidase in vacuoles, Plant J. 45 (2006) 133–143, http://dx.doi.org/10.1111/j.1365-313X.2005.02625.x.
[28] L.T. Tran, C.P. Constabel, The polyphenol oxidase gene family in poplar: phylogeny, differential expression and identification of a novel, vacuolar isoform, Planta 234 (2011) 799–813, http://dx.doi.org/10.1007/s00425-011-1441-9.
[29] L.T. Tran, J.S. Taylor, C.P. Constabel, The polyphenol oxidase gene family in land plants: lineage-specific duplication and expansion, BMC Genomics 13 (2012) 395, http://dx.doi.org/10.1186/1471-2164-13-395.
[30] S. Chang, J. Puryear, J. Cairney, A simple and efficient method for isolating RNA from pine trees, Plant Mol. Biol. Report. 11 (1993) 113–116, http://dx.doi.org/10.1007/BF02670468.
[31] L. Jaakola, a M. Pirttilä, M. Halonen, a Hohtola, Isolation of high quality RNA from bilberry (Vaccinium myrtillus L.) fruit, Mol. Biotechnol. 19 (2001) 201–203, http://dx.doi.org/10.1385/MB:19:2:201.
[32] T. Nakagawa, T. Kurose, T. Hino, K. Tanaka, M. Kawamukai, Y. Niwa, K. Toyooka, K. Matsuoka, T. Jinbo, T. Kimura, Development of series of gateway binary vectors, pGWBs, for realizing efficient construction of fusion genes for plant transformation, J. Biosci. Bioeng. 104 (2007) 34–41, http://dx.doi.org/10.1263/jbb.104.34.
[33] B.K. Nelson, X. Cai, A. Nebenführ, A multicolored set of in vivo organelle markers for co-localization studies in Arabidopsis and other plants, Plant J. 51 (2007) 1126–1136, http://dx.doi.org/10.1111/j.1365-313X.2007.03212.x.
[34] I.A. Sparkes, J. Runions, A. Kearns, C. Hawes, Rapid, transient expression of fluorescent fusion proteins in tobacco plants and generation of stably transformed plants, Nat. Protoc. 1 (2006) 2019–2025, http://dx.doi.org/10.1038/nprot.2006.286.
[35] T.C. Baldwin, M.G. Handford, M.I. Yuseff, A. Orellana, P. Dupree, Identification and characterization of GONST1, a golgi-localized GDP-mannose transporter in Arabidopsis, Plant Cell 13 (2001) 2283–2295, http://dx.doi.org/10.1105/tpc.010247.
[36] S. Bolte, F.P. Cordelieres, A guided tour into subcellular colocalisation analysis in light microscopy, J. Microsc. 224 (2006) 13–232, http://dx.doi.org/10.1111/j.1365-2818.2006.01706.x.
[37] T.N. Petersen, S. Brunak, G. von Heijne, H. Nielsen, SignalP 4.0: discriminating signal peptides from transmembrane regions, Nat. Methods 8 (2011) 785–786, http://dx.doi.org/10.1038/nmeth.1701.
[38] H. Bannai, Y. Tamada, O. Maruyama, K. Nakai, S. Miyano, Extensive feature detection of N-terminal protein sorting signals, Bioinformatics 18 (2002) 298–305, http://dx.doi.org/10.1093/bioinformatics/18.2.298.
[39] O. Emanuelsson, H. Nielsen, S. Brunak, G. von Heijne, Predicting subcellular localization of proteins based on their N-terminal amino acid sequence, J. Mol. Biol. 300 (2000) 1005–1016, http://dx.doi.org/10.1006/jmbi.2000.3903.
[40] A. Höglund, P. Dönnes, T. Blum, H.W. Adolph, O. Kohlbacher, MultiLoc: prediction of protein subcellular localization using N-terminal targeting sequences, sequence motifs and amino acid composition, Bioinformatics 22 (2006) 1158–1165, http://dx.doi.org/10.1093/bioinformatics/btl002.
[41] O. Emanuelsson, H. Nielsen, G. Von Heijne, ChloroP, a neural network-based method for predicting chloroplast transit peptides and their cleavage sites, Protein Sci. 8 (1999) 978–984, http://dx.doi.org/10.1110/ps.8.5.978.
[42] A. Krogh, B. Larsson, G. von Heijne, E.L. Sonnhammer, Predicting transmembrane protein topology with a hidden markov model: application to complete genomes11edited by F. Cohen, J. Mol. Biol. 305 (2001) 567–580, http://dx.doi.org/10.1006/jmbi.2000.4315.
[43] C. Steentoft, S.Y. Vakhrushev, H.J. Joshi, Y. Kong, M.B. Vester-Christensen, K.T.-B.G. Schjoldager, K. Lavrsen, S. Dabelsteen, N.B. Pedersen, L. Marcos-Silva, R. Gupta, E. Paul Bennett, U. Mandel, S. Brunak, H.H. Wandall, S.B. Levery, H. Clausen, Precision mapping of the human O-GalNAc glycoproteome through SimpleCell technology, EMBO J. 32 (2013) 1478–1488, http://dx.doi.org/10.1038/emboj.2013.79.
[44] P. Munoz, L. Norambuena, A. orellana, evidence for a UDP-glucose transporter in Golgi apparatus-derived vesicles from pea and its possible role in polysaccharide biosynthesis, Plant Physiol. 112 (1996) 1585–1594.
[45] B.M. Moore, W.H. Flurkey, Sodium dodecyl sulfate activation of a plant polyphenoloxidase, J. Biol. Chem. 265 (1990) 4982–4989.
[46] J. Nagahashi, A.P. Kane, Triton-stimulated nucleoside diphosphatase activity: subcellular localization in corn root homogenates, Protoplasma 112 (1982) 167–173, http://dx.doi.org/10.1007/BF01284090.
[47] B.N. Ames, [10] Assay of inorganic phosphate, total phosphate and phosphatases, Methods Enzymol. 8 (1966) 115–118, http://dx.doi.org/10.1016/0076-6879(66)08014-5.
[48] K. Wienecke, R. Glas, D.G. Robinson, Organelles involved in the synthesis and transport of hydroxyproline-containing glycoproteins in carrot root discs, Planta 155 (1982) 58–63.
[49] D.E. Titus, D. Hondred, W.M. Becker, Purification and characterization of hydroxypyruvate reductase from cucumber cotyledons, Plant Physiol. 72 (1983) 402–408, http://dx.doi.org/10.1104/pp.72.2.402.
[50] G.E. Schaller, N.D. DeWitt, Analysis of the H + ATPase and other proteins of the arabidopsis plasma membrane, Methods Cell Biol. 50 (1995) 129–148, http://dx.doi.org/10.1016/S0091-679X(08)61027-4.
[51] P.K. Smith, R.I. Krohn, G.T. Hermanson, A.K. Mallia, F.H. Gartner, M.D. Provenzano, E.K. Fujimoto, N.M. Goeke, B.J. Olson, D.C. Klenk, Measurement of protein using bicinchoninic acid, Anal. Biochem. 150 (1985) 76–85, http://dx.doi.org/10.1016/0003-2697(85)90442-7.
[52] K.S. Dhugga, S.C. Tiwari, P.M. Ray, A reversibly glycosylated polypeptide (RGP1) possibly involved in plant cell wall synthesis: purification, gene cloning, and trans-Golgi localization, Plant Biol. 94 (1997) 7679–7684, http://dx.doi.org/10.1073/pnas.94.14.7679.
[53] S. Munro, H.R.B. Pelham, An hsp70-like protein in the ER: Identity with the 78 kd glucose-regulated protein and immunoglobulin heavy chain binding protein, Cell 46 (1986) 291–300, http://dx.doi.org/10.1016/0092-8674(86)90746-4.
[54] H. Towbin, T. Staehelin, J. Gordon, Electrophoretic transfer of proteins from polyacrylamide gels to nitrocellulose sheets: procedure and some applications, Proc. Natl. Acad. Sci. U. S. A. 76 (1979) 4350–4354, http://dx.doi.org/10.1002/bies.950190612.
[55] V. De Pino, M. Borán, L. Norambuena, M. González, F. Reyes, A. Orellana, S. Moreno, Complex formation regulates the glycosylation of the reversibly glycosylated polypeptide, Planta 226 (2007) 335–345, http://dx.doi.org/10.1007/s00425-007-0485-3.
[56] T. Connolly, P. Collins, R. Gilmore, Access of proteinase K to partially translocated nascent polypeptides in intact and detergent-solubilized membranes, J. Cell Biol. 108 (1989) 299–307.
[57] M. Nishimura, D. Graham, T. Akazawa, Isolation of intact chloroplasts and other cell organelles from spinach leaf protoplasts, Plant Physiol. 58 (1976) 309–314, http://dx.doi.org/10.1104/pp.58.3.309.
[58] T. Takabe, M. Nishimura, T. Akazawa, Isolation of intact chloroplasts from spinach Spinacia-Oleracea cultivar kyoho leaf by centrifugation in gradients of the modified silica percoll, Agric. Biol. Chem. 43 (1979) 2137–2142, http://dx.doi.org/10.1080/00021369.1979.10863766.
[59] L. Orcl, M. Tagaya, M. Amherdt, A. Perrelet, J.G. Donaldson, J. Lippincott-Schwartz, R.D. Klausner, J.E. Rothman, A. Brefeldin, a drug that blocks secretion, prevents the assembly of non-clathrin-coated buds on Golgi cisternae, Cell 64 (1991) 1183–1195, http://dx.doi.org/10.1016/0092-8674(91)90273-2.
[60] V.R. Ordenes, F.C. Reyes, D. Wolff, A. Orellana, A thapsigargin-sensitive Ca(2+) pump is present in the pea Golgi apparatus membrane, Plant Physiol. 129 (2002) 1820–1828, http://dx.doi.org/10.1104/pp.002055.
[61] E. Valero, M. García-Moreno, R. Varón, F. García-Carmona, Time-dependent inhibition of grape polyphenol oxidase by tropolone, J. Agric. Food Chem. 39 (1991) 1043–1046.
[62] J.D. Sterling, H.F. Quigley, A. Orellana, D. Mohnen, The catalytic site of the pectin biosynthetic enzyme alpha-1, 4-galacturonosyltransferase is located in the lumen of the Golgi, Plant Physiol. 127 (2001) 360–371, http://dx.doi.org/10.1104/pp.127.1.360.
[63] M. Handford, C. Rodríguez-Furlán, L. Marchant, M. Segura, D. Gómez, E. Alvarez-Buylla, G.Y. Xiong, M. Pauly, A. Orellana, Arabidopsis thaliana AtUTr7 encodes a golgi-localized UDP-glucose/UDP-galactose transporter that affects lateral root emergence, Mol. Plant. 5 (2012) 1263–1280, http://dx.doi.org/10.1093/mp/sss074.
[64] C. Rautengarten, B. Ebert, I. Moreno, H. Temple, T. Herter, B. Link, D. Doñas-Cofré, A. Moreno, S. Saéz-Aguayo, F. Blanco, J.C. Mortimer, A. Schultink, W.-D. Reiter, P. Dupree, M. Pauly, J.L. Heazlewood, H.V. Scheller, A. Orellana, The Golgi localized bifunctional UDP-rhamnose/UDP-galactose transporter family of Arabidopsis, Proc. Natl. Acad. Sci. U. S. A. 111 (2014) 11563–11568, http://dx.doi.org/10.1073/pnas.1406073111.
[65] D. Utz, M. Handford, VvGONST-A and vvGONST-B are Golgi-localised GDP-sugar transporters in grapevine (Vitis vinifera L.), Plant Sci. 231 (2015) 191–197, http://dx.doi.org/10.1016/j.plantsci.2014.11.009.
[66] S. Saez-Aguayo, C. Rautengarten, H. Temple, D. Sanhueza, T. Ejsmentewicz, O. Sandoval-Ibañez, D. Doñas, J.P. Parra-Rojas, B. Ebert, A. Lehner, J.-C. Mollet, P. Dupree, H.V. Scheller, J.L. Heazlewood, F.C. Reyes, A. Orellana, UUAT1 is a Golgi-localized UDP-uronic acid transporter that modulates the polysaccharide composition of arabidopsis seed mucilage, Plant Cell 29 (2017) 129–143, http://dx.doi.org/10.1105/tpc.16.00465.
[67] C. Ritzenthaler, A. Nebenführ, A. Movafeghi, C. Stussi-Garaud, L. Behnia, P. Pimpl, L.A. Staehelin, D.G. Robinson, Reevaluation of the effects of brefeldin a on plant cells using tobacco bright yellow 2 cells expressing Golgi-targeted green fluorescent protein and COPI antisera, Plant Cell 14 (2002) 237–261, http://dx.doi.org/10.1105/tpc.010237.
[68] C. Saint-Jore-Dupas, A. Nebenfuhr, A. Boulaflous, M.-L. Follet-Gueye, C. Plasson, C. Hawes, A. Driouich, L. Faye, V. Gomord, Plant *N*-glycan processing enzymes employ different targeting mechanisms for their spatial arrangement along the secretory pathway, Plant Cell 18 (2006) 3182–3200, http://dx.doi.org/10.1105/tpc.105.036400.
[69] M.E. Arias, M. Arenas, J. Rodríguez, J. Soliveri, A.S. Ball, M. Hernández, Kraft pulp biobleaching and mediated oxidation of a nonphenolic substrate by laccase from Streptomyces cyaneus CECT 3335, Appl. Environ. Microbiol. 69 (2003) 1953–1958, http://dx.doi.org/10.1128/AEM.69.4.1953-1958.2003.
[70] V. Kahn, A. Andrawis, Inhibition of mushroom tyrosinase by tropolone, Phytochemistry 24 (1985) 905–908, http://dx.doi.org/10.1016/S0031-9422(00)83150-7.
[71] B. Paul, L.R. Gowda, Purification and characterization of a polyphenol oxidase from the seeds of field bean (Dolichos lablab), J. Agric. Food Chem. 48 (2000)

3839–3846, http://dx.doi.org/10.1021/jf000296s.
[72] T. Nakayama, K. Yonekura-Sakakibara, T. Sato, S. Kikuchi, Y. Fukui, M. Fukuchi-Mizutani, T. Ueda, M. Nakao, Y. Tanaka, T. Kusumi, T. Nishino, Aureusidin synthase a polyphenol oxidase homolog responsible for flower coloration, Science (80-.) 290 (2000) 1163–1166, http://dx.doi.org/10.1126/science.290.5494.1163.
[73] M.L. Sullivan, Beyond brown: polyphenol oxidases as enzymes of plant specialized metabolism, Front. Plant Sci. 5 (2015) 783, http://dx.doi.org/10.3389/fpls.2014.00783.
[74] T. Nakatsuka, E. Yamada, H. Takahashi, T. Imamura, M. Suzuki, Y. Ozeki, I. Tsujimura, M. Saito, Y. Sakamoto, N. Sasaki, M. Nishihara, Genetic engineering of yellow betalain pigments beyond the species barrier, Sci. Rep. 3 (2013) 1970, http://dx.doi.org/10.1038/srep01970.
[75] D. Wahler, C.S. Gronover, C. Richter, F. Foucu, R.M. Twyman, B.M. Moerschbacher, R. Fischer, J. Muth, D. Prüfer, Polyphenoloxidase silencing affects latex coagulation in Taraxacum species, Plant Physiol. 151 (2009) 334–346, http://dx.doi.org/10.1104/pp.109.138743.
[76] E. Grotewold, The challenges of moving chemicals within and out of cells: insights into the transport of plant natural products, Planta 219 (2004) 906–909, http://dx.doi.org/10.1007/s00425-004-1336-0.
[77] J. Zhao, R.A. Dixon, The ins and outs of flavonoid transport, Trends Plant Sci. 15 (2010) 72–80, http://dx.doi.org/10.1016/j.tplants.2009.11.006.
[78] F. Poustka, N.G. Irani, A. Feller, Y. Lu, L. Pourcel, K. Frame, E. Grotewold, A trafficking pathway for anthocyanins overlaps with the endoplasmic reticulum-to-vacuole protein-sorting route in Arabidopsis and contributes to the formation of vacuolar inclusions, Plant Physiol. 145 (2007) 1323–1335, http://dx.doi.org/10.1104/pp.107.105064.
[79] T. Ichino, K. Fuji, H. Ueda, H. Takahashi, Y. Koumoto, J. Takagi, K. Tamura, R. Sasaki, K. Aoki, T. Shimada, I. Hara-Nishimura, GFS9/TT9 contributes to intracellular membrane trafficking and flavonoid accumulation in Arabidopsis thaliana, Plant J. 80 (2014) 410–423, http://dx.doi.org/10.1111/tpj.12637.
[80] J. Zhao, Flavonoid transport mechanisms: how to go, and with whom, Trends Plant Sci. 20 (2015) 576–585, http://dx.doi.org/10.1016/j.tplants.2015.06.007.
[81] Y. Wang, M. Chantreau, R. Sibout, S. Hawkins, Plant cell wall lignification and monolignol metabolism, Front. Plant Sci. 4 (2013) 220, http://dx.doi.org/10.3389/fpls.2013.00220.
[82] H.T. Parsons, K. Christiansen, B. Knierim, A. Carroll, J. Ito, T.S. Batth, A.M. Smith-Moritz, S. Morrison, P. McInerney, M.Z. Hadi, M. Auer, A. Mukhopadhyay, C.J. Petzold, H.V. Scheller, D. Loque, J.L. Heazlewood, Isolation and proteomic characterization of the Arabidopsis Golgi defines functional and novel components involved in plant cell wall biosynthesis, Plant Physiol. 159 (2012) 12–26, http://dx.doi.org/10.1104/pp.111.193151.